ROMANIAN JOURNAL OF INFORMATION SCIENCE AND TECHNOLOGY
Volume 27, Number 3–4, 2024, 255–266

Dimension-Reduced Modeling for Local Volatility Surface via Unsupervised Learning

Zheng-Liang LU[1] and U Hou LOK[2,*]

[1]Department of Computer Science & Information Engineering, National Taiwan University, No. 1, Sec. 4, Roosevelt Rd., Taipei, Taiwan

[2]Department of Accounting Information, National Taipei University of Business, No. 321, Sec. 1, Jinan Rd, Taipei 10051, Taiwan.

Email: d00922011@ntu.edu.tw, miguellok@ntub.edu.tw*

* Corresponding author

Abstract. Volatility is a key factor for option pricing. It displays skewness across different strike prices and maturity days when implied by the Black-Scholes formula. This phenomenon is called the volatility smile. The local volatility model is popular because it fits this smile. It assumes the volatilities a deterministic function of underlying asset and time. These volatilities form the local volatility surface (LVS). LVS evolves over time and this dynamics can be high-dimensional and fluctuating. In this research, we show that the LVS may be described by a small number of orthogonal factors. This is accomplished by studying the LVS dynamics with time series data on option prices and extracting their essences via principal component analysis (PCA) and multilinear PCA (MPCA). We aim at recognizing these dominant components. In this case, the dimensions of LVS are reduced, and these dominant components are used to reconstruct the LVS. Numerical results show that the reconstructed LVS retains the important characteristics while filtering out noise well. In particular, over 80% of observations are within 10% in the maximum absolute relative difference (MARD). Moreover, MPCA provides an extra degree of freedom for reconstruction as well as interpretation because it preserves the tensor structure.

Key-words: Dimension reduction; implied volatilities; local volatility surfaces; multilinear principal component analysis; unsupervised learning.

1. Introduction

Volatility is a crucial factor in option pricing. It can be estimated from the market option prices via some option pricing models. Black-Scholes (BS) model is one of the most famous option pricing models [1]. The volatilities implied by the market option prices via BS model is called the implied volatility. The implied volatility displays skewness in underlying strike prices and times to maturity – the so-called "volatility smile" phenomenon and widely observed in many derivative markets [2]. These implied volatilities across strike prices and times to maturity form the implied volatility surface (IVS). However, the IVS often needs to be re-calibrated with market options because these options change over time. The time series of IVS forms the term structure of IVS, or say the IVS dynamics. IVS dynamics can be categorized as a nonlinear modeling and estimation problem. In this domain, many effective methods have been proposed including extended Kalman filter [3], tensor product-based model transformation [4], continuous-discrete filtering [5], and neural network [6, 7]. These methods are tailored to address specific applications and scenarios.

The high-dimensional IVS dynamics can be represented with a parsimonious model by dimension reduction [8]. Principal component analysis (PCA) is a popular unsupervised learning technique for dimension reduction. Its main idea is to seek orthonormal bases (principal components) for the original observations in the directions with maximum variances [9]. In the scenario of IVS dynamics, the directions with maximum variance distinguish systematic risk from idiosyncratic shocks [10]. PCA has been applied successfully in analyzing the term structure of interest rates [11, 12]. Many works discuss the performance of PCA on the IVS dynamics [13, 14, 15]. Traditionally, PCA first vectorizes the tensor data and proceeds with the eigenvalue decomposition with a large covariance matrix. This might break the original 4-dimensional structure. So, a tensor version of PCA that preserves the tensor structure may have some advantages. Multilinear PCA (MPCA) is such one that preserves the natural tensor structure of IVS dynamics in searching of principal components [16]. Thus, MPCA might alleviate the negative impact of high dimensionality and improve prediction and estimation performances. It can be applied in various domains such as spectral analysis, nonlinear modeling, communication and radar processing, image processing, biomedical applications, etc [17]. The MPCA applied in IVS dynamics is firstly found in [18]. Their investigation shows that tensor structure performs better in tracking between the eigenportfolio and the weighted IVS returns portfolio.

While IVS is derived from market option prices, albeit with necessary regularization, it primarily serves as a trading metric rather than a comprehensive model. It cannot be used directly for exotic option pricing and hedging. Some smile-consistent models are needed. The local volatility (LV) model is such a model which extends the BS model and is capable to capture the volatility smile. It assumes the instantaneous volatility as a deterministic function of the stock price and time [2, 19, 20]. This assumption makes the LV model preference-free, like the BS model. So the market is complete and options can be valued by no-arbitrage argument without the market price of risk [21]. The local volatilities across different underlying asset prices and time form the LV surfaces (LVS). In general, the LVS is more volatile than IVS as the latter can be viewed as some kind of average the former [10, 22]. The LVS can be obtained by the market option prices via the Dupire's equation [19].

To the best of the authors' knowledge, there is still no literature to investigate the LVS dynamics via PCA. As LVS is a very popular model for exotic option pricing and hedging compatible with the market prices of vanilla options, it is essential to extract the dominating features of the LVS so that systematic risk can be distinguished from idiosyncratic shocks. For this purpose,

PCA and MPCA are applied to the LVS dynamics for dimension reduction in this research. Our results show that the LVS may be described by a small number of orthogonal factors and thus constrained to a much lower dimension. This may be the first research to accomplish this goal. Moreover, as MPCA preserves the tensor structure of LVS, it provides an extra degree of freedom for reconstruction and interpretation via its left and right eigenvectors. The methodology in this research can be applied to improve option pricing and risk hedging.

Our paper is organized as follows. The IVS and LVS are briefly presented in Section 2. Section 3 provides the methodologies for the dimension reduction of IVS and LVS via PCA and MPCA. Numerical results for our approach are given in Section 4. Section 5 concludes this paper.

2. Implied Volatility Surface (IVS) and Local Volatility Surface (LVS)

In this section, we briefly review both IVS and LVS. Suppose the underlying asset price evolves according to the following geometric Brownian motion:

$$\frac{dS_t}{S_t} = (r-q)dt + \sigma dW_t, \tag{1}$$

where t is time, S_t is underlying asset price at t, r is the risk-free rate, q is the dividend of the underlying asset, σ is asset's volatility and W_t is the standard Brownian motion. This is the celebrated Black-Scholes model [1]. From this model, one can deduce the Black–Scholes formula, which gives a theoretical estimate of the price of European-style options. The value of the call option is

$$\begin{aligned} \text{Call}(S_t,t) &= N(d_1)S_t - N(d_2)Ke^{-r(T-t)}, \\ \text{where} \quad d_1 &= \frac{1}{\sigma\sqrt{T-t}}\left[\ln\frac{S_t}{K} + (r+\frac{\sigma^2}{2})(T-t)\right], \\ d_2 &= d_1 - \sigma\sqrt{T-t}, \end{aligned} \tag{2}$$

and K is the strike price and $N(\cdot)$ is standard normal cdf. Similarly, the put option is

$$\text{Put}(S_t,t) = N(-d_2)Ke^{-r(T-t)} - N(-d_1)S_t. \tag{3}$$

With the call and put values read from the financial market, the volatility σ can be obtained by the inversing Eqs. (2) or (3). The volatilities implied by the market prices of call or put via Eqs. (2) or (3), respectively, are called the implied volatilities. In practice, the market prices of call and put show the dependency on many factors including strike price and maturity day. The variation of implied volatilities across strike prices and maturity days forms the implied volatility surface (IVS).

As the market data of implied volatilities are discrete, interpolation and smoothing are needed to form the IVS. Gaussian kernel is applied in smoothing, which is a non-parametric smoothing technique that captures the IVS pattern better than the parametric one [14]. The smooth estimator of IVS is expressed as

$$\widehat{\text{IVS}}_t(K,T) = \frac{\sum_{\ell=1}^{m}\text{IVS}_t(K_\ell,T_\ell)g(K-K_\ell,T-T_\ell)}{\sum_{\ell=1}^{m}g(K-K_\ell,T-T_\ell)}, \tag{4}$$

where m is the number of options traded on that day, $g(x,y) = \frac{1}{2\pi}[e^{(-x^2/2h_1)}e^{(-y^2/2h_2)}]$ is a Gaussian kernel with bandwidth parameters h_1 and h_2. Gaussian smoothing outputs a 'weighted average' of each data point's neighbors. It provides gentler smoothing and preserves edges. The weight is defined by the kernel in the way that closer points have higher weights. Gaussian kernel with suitable bandwidths filters out the noises while preserving the market information.

For any particular time, an IVS is obtained from the market option prices. As time evolves, a time series of such IVS, or, say, IVS dynamics, are generated. The IVS dynamics are often used in hedging and scenario analysis in risk management. In general, IVS is a complex, high-dimensional object. Past literature shows that it is possible to describe the IVS dynamics with a small number of factors, thus in a much lower dimensions, so that the essences of the IVS can be retained and the noise can be filtered out [14, 15].

Implied volatility is viewed as a kind of metric in trading, it is not a suitable model for options with volatility smile. In this case, smile-consistent models are needed. The LV model is such a model that assumes the instantaneous volatility to be a deterministic function of the underlying asset price and time [2, 19, 20]. This assumption makes the LV model preference-free. In this case, the market is complete and options can be priced by the standard no-arbitrage argument without the market price of risk [21]. The LV model is expressed as:

$$\frac{dS_t}{S_t} = (r-q)dt + \sigma(S,t)dW_t, \tag{5}$$

where t is the time, S_t is underlying asset price at t, r is the risk-free interest rate, q is the dividend of the underlying asset, σ is the asset's volatility and W_t is the standard Brownian motion. Eq. (5) represents the evolution of the instantaneous volatility along the market expectation at the moment. The LV model is commonly used to price and hedge vanilla and exotic options.

The local volatilities $\sigma(S,t)$ in Eq. (5) are not directly observable from the market. Instead, they are constructed via the observed option prices. There are a few ways to calibrate the local volatilities from the option prices or implied volatilities in the market. Trees and Dupire's equation are two common ways [19, 20, 23]. The Dupire's equation below is expressed in terms of option prices [10]:

$$\sigma^2_{K,T}(S_t,t) = 2\frac{\frac{\partial P_t(K,T)}{\partial T} + qP_t(K,T) + (r-q)K\frac{\partial P_t(K,T)}{\partial K}}{K^2\frac{\partial^2 P_t(K,T)}{\partial K^2}}, \tag{6}$$

where P_t is the option price at time t, K is the strike price of the underlying asset. The local volatilities $\sigma^2_{K,T}(S_t,t)$ in Eq. (6) across different time t and underlying asset prices S_t form the LV surface (LVS). In general, the LVS can be much more fluctuating compared to IVS since IVS is some kind of average of the former [10, 22]. In practice, only a limited number of options are traded in the market; thus interpolation, extrapolation, and even smoothing are needed. An essential property of an LVS is that the surface should be arbitrage-free. A possible approach is by implied tree with interpolation. Another promising approach to meet this goal is proposed in [24]. They apply the implicit finite difference method to interpolate and extrapolate market options to guarantee that the LVS is arbitrage-free. Their algorithm will be used to generate the LVS in this research.

3. Dimension Reduction for LVS via PCA and MPCA

Local volatilities can be obtained with the market option prices across different strike prices and maturity days by Eq. (6). Then an arbitrage-free LVS can be built with the interpolation algorithm in [24]. Market option prices evolve with time, so LVS also changes accordingly and forms the LVS dynamics. In practice, LVS is high-dimensional, accompanied by significant noise, reflecting the financial markets' tendencies to overreact or underreact to exceptional events, which cannot be fully explained. Fortunately, the essential characteristics, such as shape, level, or slope, can be identified by studying the deformation of LVS from its dynamics. These factors are expected to capture the systematic risks and filter out the idiosyncratic shocks. PCA is a popular unsupervised learning method to identify underlying patterns and reduce the dimensions of the dataset with minimal loss of information. This is achieved by the eigenvalue decomposition of the dataset's covariance matrix.

However, traditional PCA for tensor objects, such as images or videos, has to reshape the tensor structure into vectors, which may result in inefficient computation for complex nonlinear relationships. MPCA overcomes such difficulty by retaining the tensor structure of observations. It aims to reduce the data dimensionality while capturing relevant multilinear relationships. In addition, it provides an extra degree of freedom for reconstruction and interpretation via its left and right eigenvectors. Here, both PCA and MPCA will be applied to the LVS dynamics to extract the important components.

We first describe the PCA for the LVS dynamics. Let the collection of matrices $\{\mathbf{X}_i \in \mathbb{R}^{p\times q}\}_{i=1}^n$ be the LVS dynamics, where i is the time step at the moment, n is the number of trading days, and p and q are the original dimensions of the underlying asset prices and time respectively. For simplicity, we assume that $\mathbf{X}_i$ has been centered. For PCA, $\mathbf{X}_i$ is vectorized, vec($\mathbf{X}_i$), to form a large matrix $\mathbf{X} = [\,\text{vec}(\mathbf{X}_1), \ldots, \text{vec}(\mathbf{X}_n)\,]^\mathsf{T}$ of size of $n \times k$, where $k = pq$. The principal components, $\mathbf{V}$, of the LVS dynamics are obtained by the singular value decomposition (SVD) procedure [9]. These $\mathbf{V}$'s are the latent factors that are the linear combinations of vec($\mathbf{X}_i$):

$$\mathbf{V}_{j,i} = \Psi_j \text{vec}(\mathbf{X}_i), \quad j \in 1, \ldots, k, \tag{7}$$

where Ψ is the loading matrix with size of $k \times k$. The j^{th} principal component is designed to encapsulate the maximum amount of variation while ensuring orthogonality to the first $j-1$ principal components. For dimension reduction, the first few J ($J << k$) principal components are preserved and the noise-filtered (dimension-reduced) LVS is constructed with the loadings Ψ,

$$\widetilde{\mathbf{X}}_{j,i} = (\Psi_{1:J,\,j})^\top \mathbf{V}_{1:J,\,i}, \quad j \in 1, \ldots, k. \tag{8}$$

Next, we describe the MPCA for the LVS dynamics. Suppose that $\tilde{p} \le p$ and $\tilde{q} \le q$ are the prespecified dimensions of underlying asset prices and time respectively, and $\|\cdot\|_F$ is the Frobenius norm. The LVS tensor is an order-2 tensor of size $p \times q$. It consists of 2 sets of orthonormal bases, or says 2 modes, one for the asset price mode of dimensionality p, and another for the time mode of dimensionality q. So one can obtain the orthonormal basis called mode-ℓ basis $\mathbf{U}_\ell$, $\ell = 1, 2$, by SVD. As the purpose of MPCA here is for dimension reduction, only a few leading columns in $\mathbf{U}_\ell$ are kept to form a partial basis. For simplicity, the LVS has assumed to be centered: $\mathbf{X}_i \leftarrow \mathbf{X}_i - \overline{X}$, where $\overline{X} = \frac{1}{n}\sum_{i=1}^n \mathbf{X}_i$. MPCA finds the best approximation of the centered LVS dynamics $\{\mathbf{X}_i \in \mathbb{R}^{p\times q}\}_{i=1}^n$ by minimizing error distance [25]:

$$\underset{\mathbf{U_1}\in\mathbb{R}^{p\times\tilde{p}},\mathbf{U_2}\in\mathbb{R}^{q\times\tilde{q}}}{\text{argmin}} \sum_{i=1}^n \|\mathbf{X}_i - \mathbf{U_1}\mathbf{U_1}^\mathsf{T}\mathbf{X}_i\mathbf{U_2}\mathbf{U_2}^\mathsf{T}\|_F^2. \tag{9}$$

Solving the above optimization problem is equivalent to solve

$$\underset{\mathbf{U_1}\in\mathbb{R}^{p\times\tilde{p}},\mathbf{U_2}\in\mathbb{R}^{q\times\tilde{q}}}{\operatorname{argmax}} \sum_{i=1}^{n} \|{\mathbf{U_1}}^{\top}\mathbf{X}_i\mathbf{U_2}\|_F^2. \tag{10}$$

Algorithm 1: MPCA Algorithm

input : Collection of centered LVS $\{\mathbf{X}_i \in \mathbb{R}^{p\times q}\}_{i=1}^{n}$, termination factor δ^*, predetermined dimension $(\tilde{p}, \tilde{q})$.

output: $\hat{\mathbf{U}}_\mathbf{1} \in \mathbb{R}^{p\times\tilde{p}}$, $\hat{\mathbf{U}}_\mathbf{2} \in \mathbb{R}^{q\times\tilde{q}}$.

initialize matrix ${\mathbf{U_1}}^{(0)} \in \mathbb{R}^{p\times\tilde{p}}$ with high order SVD [28].
Set t=0 and $\delta = 2\delta^*$.
while $\delta > \delta^*$ **do**
  find ${\mathbf{U_2}}^{(t+1)} = (\mathbf{u}_{21}, \mathbf{u}_{22}, \ldots, \mathbf{u}_{2\tilde{q}})$, where $\mathbf{u}_{2i}$'s are the leading $\tilde{q}$ eigenvectors of

$$\sum_{i=1}^{n} \left(\mathbf{X}_i^{\top}{\mathbf{U_1}}^{(t)}{{\mathbf{U_1}}^{(t)}}^{\top}\mathbf{X}_i\right).$$

  find ${\mathbf{U_1}}^{(t+1)} = (\mathbf{u}_{11}, \mathbf{u}_{12}, \ldots, \mathbf{u}_{1\tilde{p}})$, where $\mathbf{u}_{1i}$'s are the leading $\tilde{p}$ eigenvectors of

$$\sum_{i=1}^{n} \left(\mathbf{X}_i{\mathbf{U_2}}^{(t+1)}{{\mathbf{U_2}}^{(t+1)}}^{\top}\mathbf{X}_i^{\top}\right).$$

  update δ:

$$\delta = \frac{1}{n}\left(\sum_{i=1}^{n} \|{{\mathbf{U_1}}^{(t+1)}}^{\top}\mathbf{X}_i{\mathbf{U_2}}^{(t+1)}\|_F^2 - \sum_{i=1}^{n} \|{{\mathbf{U_1}}^{(t)}}^{\top}\mathbf{X}_i{\mathbf{U_2}}^{(t)}\|_F^2\right).$$

  $t = t + 1$.
end
return $\hat{\mathbf{U}}_\mathbf{1} = {\mathbf{U_1}}^{(t)}$ & $\hat{\mathbf{U}}_\mathbf{2} = {\mathbf{U_2}}^{(t)}$.

The aim of Eq. (10) is to find the left and right principal components $\mathbf{U_1}$ and $\mathbf{U_2}$ iteratively. As it is not trivial to solve the projection matrix $\mathbf{U_1}$ and $\mathbf{U_2}$, an iterative optimization procedure is used instead [9]. The procedure is shown in Algorithm 1, and the projection matrix are thus obtained. The noise-filtered (dimension-reduced) LVS can then be constructed by $\widetilde{\mathbf{X}}_i = \hat{\mathbf{U}}_\mathbf{1}^{\top}\mathbf{X}_i\hat{\mathbf{U}}_\mathbf{2}$. The convergence of $({\mathbf{U_1}}^{(t)}, {\mathbf{U_2}}^{(t)})$ ensure that $\lim_{t\to\infty}({\mathbf{U_1}}^{(t)}, {\mathbf{U_2}}^{(t)})$ is a local maximum point [9]. It is likely to obtain a global maximum point with a wisely chosen initial value. As the solution of high order SVD is marginally optimal in each mode of the ℓ-mode bases. So it is recommended to initialize ${\mathbf{U_1}}^{(0)}$ with high order SVD as in Algorithm 1. With $\mathbf{U_1}$ and $\mathbf{U_2}$, the dimension-reduced LVS will be constructed and its characteristics will be investigated with Taiwan market data in the next section. For comparison, the IVS dynamics are also studied as LVS is generally more volatile than IVS.

4. Numerical Results for Taiwan Weighted Exchange Index Derivative Market

In this section, dimension reduction is performed for the LVS generated by the European-style options traded in the Taiwan weighted exchange index derivative market. Our dataset is sourced from Taiwan Economic Journal, containing daily European calls and puts [27]. The time spans from Jan., 04, 2021 to Dec., 31, 2021, resulting in a total of 244 trading days with 148,191 call and put option contracts. The data with maturity days less than two weeks are excluded due to the well-known stability issue for short maturity. For each trading day, both calls and puts across different strike prices and maturity days are used to generate the IVS. After performing interpolation, each IVS is of size 31×30. Similarly, the local volatilities in every trading day are obtained via the Dupire's equation with the calls and puts at that day. Then arbitrage-free LVS are generated with the interpolation algorithm in [24]. A series of such daily IVS and LVS are used to perform dimension reduction via PCA and MPCA in Section 3.

We first demonstrate the variances accounted by the dominating principal components via PCA. Four types of volatility surfaces are discussed here: IVS, differential IVS, LVS, and differential LVS. The differential IVS (LVS) is the variation of the IVS (LVS) for two consecutive trading days. The results via PCA are shown in Table 1. The leading three principal components account for about 80% of variance. Our results on IVS align with the findings in [14]. They suggest that the IVS dynamics of both the S&P500 index options and the FTSE 100 index options can be adequately captured by the first three principal components [14]. Our IVS results confirm that the recent Taiwan Index option market can also be described approximately by these three components. We proceed to discuss the LVS results via PCA. The leading three principal components account for about 60%–70% of variance of LVS. This is not quite surprising, as the LVS exhibits significantly higher levels of fluctuation compared to the IVS. The tensor structure of LVS can be more intricate compared with that of IVS. So it may be beneficial to retain its tensor structure while searching for principal components, as it mitigates the adverse influence of high dimensionality and leads to efficiency gain in estimation. Moreover, another advantage of MPCA over traditional PCA is an extra degree of freedom for reconstruction and interpretation provided by the left and right eigenvectors. MPCA will be applied to the LVS and, for comparison, to the IVS as well.

Table 1. Variances accounted by the first three principal components for IVS and LVS via PCA

Input Surface	1	2	3
IVS	56.65%	20.87%	6.46%
Differential IVS	60.63%	11.06%	9.78%
LVS	52.41%	12.07%	8.32%
Differential LVS	39.66%	12.03%	9.02%

Table 2. Variances accounted by the first three left and right principal components for IVS via MPCA.

left / right	1	2	3
1	36.36%	16.38%	2.56%
2	13.80%	10.22%	2.62%
3	5.70%	4.00%	1.23%

Table 3. Variances accounted by the first three left and right principal components for differential IVS via MPCA.

left / right	1	2	3
1	47.32%	10.75%	2.43%
2	11.34%	12.37%	3.61%
3	2.20%	2.08%	0.71%

Table 4. Variances accounted by the first three left and right principal components for LVS via MPCA.

left / right	1	2	3
1	29.78%	11.10%	3.70%
2	19.15%	8.11%	2.46%
3	10.76%	5.25%	1.77%

Table 5. Variances accounted by the first three left and right principal components for differential LVS via MPCA.

left / right	1	2	3
1	30.28%	10.74%	4.25%
2	27.16%	7.49%	2.72%
3	3.82%	2.74%	1.41%

We first apply MPCA to the IVS and the differential IVS. The variance explained by each left and right eigenvector, up to the first nine eigenvectors, is provided in Tables 2 and 3 respectively. Our results indicate that the first three left and right eigenvectors collectively account for over 90% of the variance within the dataset. Furthermore, the three most significant components alone explain about 67% of the total variance. Next, the performances of the MPCA on the LVS and differential LVS are shown in Tables 4 and 5 respectively. The first three left and right eigenvectors capture about 90% of the variance of both LVS and differential LVS. The three most significant components explain about 60%–68% of the total variance. Though the results are not greatly improved compared to those in PCA, MPCA provides an extra degree of freedom to reconstruct the dimension-reduced LVS as well as enhance its interpretability along its 2 modes. The surfaces formed by the leading two left and right eigenvectors are presented in Fig. 1.

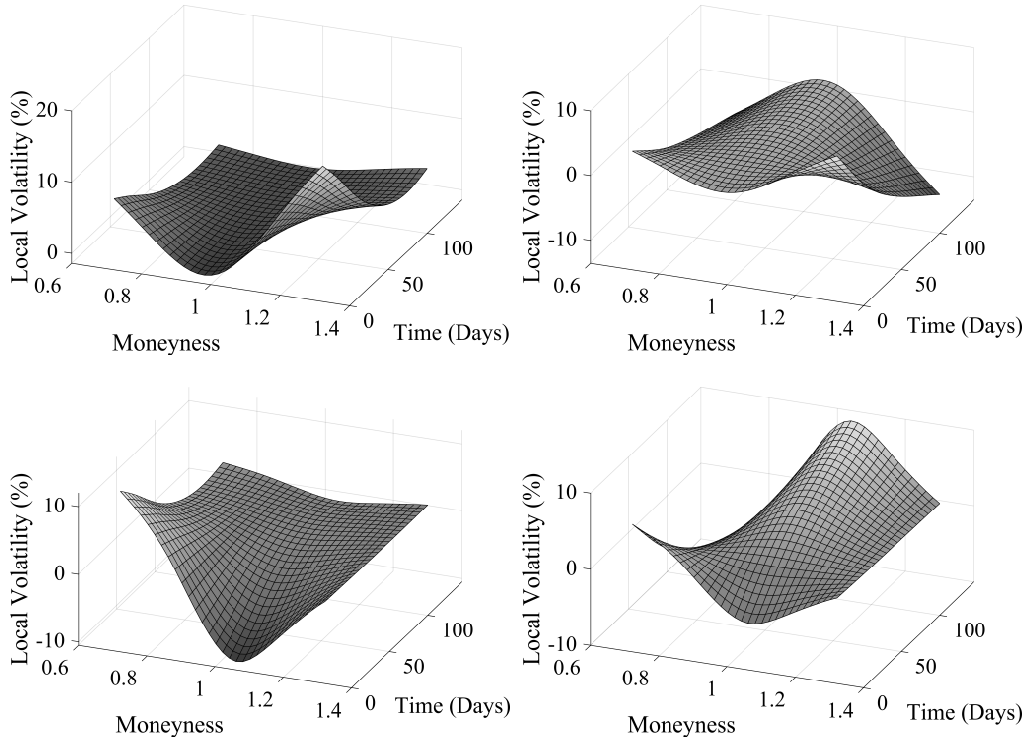

Fig. 1. The shapes of eigenvectors of LVS via MPCA. Moneyness is the underlying asset price divided by the strike price. Top Left: 1st left and 1st right eigenvectors. Top Right: 1st left and 2nd right eigenvectors. Bottom Left: 2nd left and 1st right eigenvectors. Bottom Right: 2nd left and 2nd right eigenvectors.

Each eigenvector captures specific characteristics of the LVS. The 1st left and 1st right eigenvector might be interpreted as the level effect. The 1st left and 2nd right, and 2nd left and 1st right eigenvectors might be viewed as some kind of slope effect along underlying asset price (moneyness) and time, respectively. The 2nd left and 2nd right eigenvectors might be considered as the cross-interaction between underlying asset price (moneyness) and time. This interaction term can possibly be viewed as the contribution of the nonlinear relationship in the LVS, a dimension that traditional PCA fails to address. It enables us to discern the contributions from various dimensions (along the modes) rather than reporting principal components without explicit information about the dimensions involved. This is another benefit of MPCA to preserve the tensor structure in dimension reduction. A parallel result holds for the differential LVS as well. Fig. 2 shows a sample LVS and its corresponding reconstructed LVS by the first three left and right principal components. They are similar to each other. To verify the performances of our approach comprehensively, we compare the differences between the reconstructed LVS and the original one with the whole dataset. The in-sample data spans from Jan., 4, 2021, to Nov., 30, 2021, while the out-of-sample data spans from Dec., 1, 2021, to Dec., 30, 2021. So, they encompass 222 days and 22 days respectively. Fig. 3 given in [28] displays the histogram of the maximum absolute relative difference (MARD) between the original LVS and the reconstructed one via MPCA. The empir-

ical distribution for the in-sample reconstructed LVS yields a median MARD of 2.58%, while that for the out-of-sample surface presents a median MARD of 7.18%. In particular, over 80% of both in-sample and out-of-sample reconstructed LVS maintain a MARD below 10%. Our empirical results confirm that the LVS dynamics maintain a long-term stable structure, reinforcing its viability for application in financial hedging strategies.

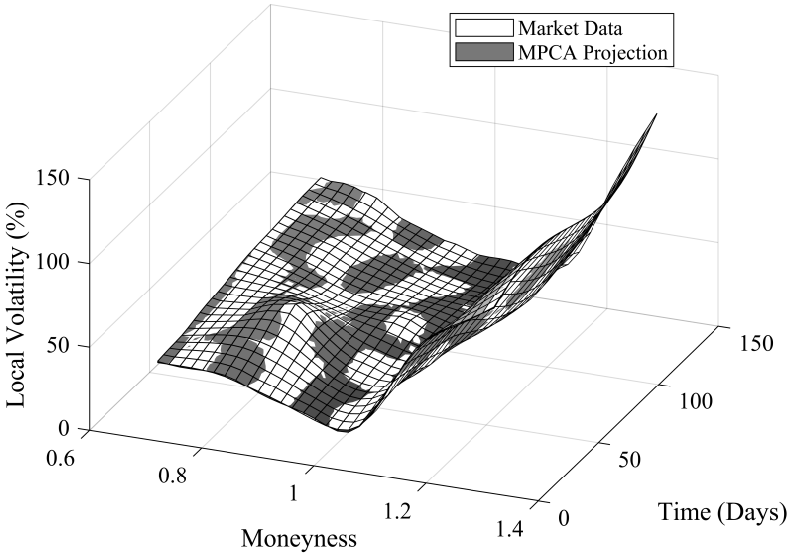

Fig. 2. An out-of-sample reconstructed LVS via the first three left and right eigen surfaces of MPCA.

5. Conclusions

There was no literature to investigate the LVS dynamics via PCA. This research employs PCA and its tensor variation, MPCA, to distill the essences of LVS dynamics. Both unsupervised learning methods aim to capture the fundamental and long-term structure of LVS while filtering out the market noise. Our empirical results confirm their effectiveness and robustness. Both in-sample and out-of-sample results show that the reconstructed LVS retains the important characteristics while filtering out noise well. Specifically, over 80% of observations fall within 10% in MARD when reconstructing LVS with the first three left and right eigenvectors. Moreover, we show that MPCA provides an extra degree of freedom to reconstruct the dimension-reduced LVS as well as enhance its interpretability because it preserves the tensor structure. The methodology in this research can be applied to improve option pricing and dynamic hedging.

Acknowledgement. This work was supported in part by the National Science and Technology Council of Taiwan under grant NSTC 112-2221-E-141-002, and in part by the Higher Education Sprout Project of the Ministry of Education of Taiwan.

References

[1] F. BLACK and M. SCHOLES, *The pricing of options and corporate liabilities*, Journal of Political Economics **81**(3), 1973, pp. 637–654.

[2] M. RUBINSTEIN, *Implied binomial tree*, Journal of Finance **49**(3), 1994, pp. 771–818.

[3] A.-I. SZEDLAK-STINEAN, R.-E. PRECUP, E. M. PETRIU, R.-C. ROMAN, E.-L. HEDREA and C.-A. BOJAN-DRAGOS, *Extended Kalman filter and Takagi-Sugeno fuzzy observer for a strip winding system*, Expert Systems with Applications **208**, 2022, paper 118215.

[4] E.-L. HEDREA, R.-E. PRECUP, R.-C. ROMAN and E. M. PETRIU, *Tensor product-based model transformation approach to tower crane systems modeling*, Asian Journal of Control **23**(3), 2021, pp. 1313–1323.

[5] R. HIRPARA, *State estimation of permanent magnet synchronous motor dynamics using higher-order continuous-discrete filtering equations*, Romanian Journal of Information Science and Technology **25**(3–4), 2022, pp. 303–321.

[6] R.-E. PRECUP, G. DUKA, S. TRAVIN and I. ZINICOVSCAIA, *Processing, neural network-based modeling of biomonitoring studies data and validation on Republic of Moldova data*, Proceedings of the Romanian Academy Series A-Mathematics Physics Technical Sciences Information Science **23**(4), 2022, pp. 403–410.

[7] K. YURTKAN, A. ADALIER and U. TEKGUC, *Student success prediction using feedforward neural networks*, Romanian Journal of Information Science and Technology **26**(2), 2023, pp. 121–136.

[8] M. FENGLER, W. HARDLE and P. SCHMIDT, *Common factors governing VDAX movements and the maximum loss*, Journal of Financial Markets and Portfolio Management **16**(1), 2002, pp. 16–29.

[9] T.-L. CHEN, S.-Y. HUANG, H. HUNG and I.-P. TU, *An introduction to multilinear principal component analysis*, Journal of the Chinese Statistical Association **52**, 2014, pp. 24–43.

[10] M. FENGLER, *Semiparametric Modeling of Implied Volatility*, Springer, Berlin, 2005.

[11] C. GOURIEROUX and J. JASIAK, *Dynamic factor nodels*, Econometrics Review **20**(4), 2001, pp. 385–424.

[12] R. REBONATO, *Interest-Rate Option Models: Understanding, Analyzing and Using Models for Exotic Interest-Rate Options*, John Wiley & Sons, Hoboken, NJ, 1998.

[13] G. SKIADOPOULOS, S. HODGES and L. CLEWLOW, *The dynamics of the S&P 500 implied volatility surface*, Review of Derivatives Research **3**(3), 2000, pp. 263–282.

[14] R. CONT and J. FONSECA, *Dynamics of implied volatility surfaces*, Quantitative Finance **2**, 2002, pp. 45–60.

[15] M. FENGLER, W. HARDLE and C. VILLA, *The dynamics of implied volatilities: A common principal components approach*, Review of Derivatives Research **6**(3), 2003, pp. 179–202.

[16] H. LU, K. N. PLATANIOTIS and A. N. VENETSANOPOULOS, *MPCA: Multilinear Principal Component Analysis of tensor objects*, IEEE Transactions on Neural Networks **19**(1), 2008, pp. 18–39.

[17] R. BADEAU and R. BOYER, *Fast Multilinear singular value decomposition for structured tensors*, SIAM Journal on Matrix Analysis and Applications **30**(3), 2008, pp. 1008–1021.

[18] M. AVELLANEDA, B. HEALY, A. PAPANICOLAOU and G. PAPANICOLAOU, *PCA for implied volatility surfaces*, Journal of Financial Data Science **2**(2), 2020, pp. 85–109.

[19] B. DUPIRE, *Pricing with a smile*, Risk **7**(1), 1994, pp. 18–20.

[20] E. DERMAN and I. KANI, *Riding on a smile*, Risk **7**(2), 1994, pp. 32–39.

[21] R. REBONATO, *Volatility and Correlation*, John Wiley & Sons, West Sussex, 2004.

[22] U H. LOK and Y.-D. LYUU, *Efficient trinomial trees for local-volatility models in pricing double-barrier options*, Journal of Futures Markets **40**(4), 2020, pp. 556–574.

[23] U H. LOK and Y.-D. LYUU, *A valid and efficient trinomial tree for general local-volatility models*, Computational Economics **60**(3), 2022, pp. 817–832.

[24] J. ANDREASEN and B. N. HUGE, *Volatility Interpolation*, 2010, Available online at `https://papers.ssrn.com/sol3/papers.cfm?abstract_id=1694972`.

[25] J. YE, *Generalized low rank approximations of natrices*, Machine Learning **61**(1–3), 2005, pp. 167–191.

[26] L. D. LATHAUWER, B. D. MOOR and J. VANDEWALLE, *A multilinear singular value decomposition*, SIAM Journal on Matrix Analysis and Applications **21**(4), 2000, pp. 1253–1278.

[27] TEJ Data Service, Retrieved from TEJ Data Service, 2023, Available online at `http://www.tej.com.tw/twsite/TEJ%E8%B3%87%E6%96%99%E5%BA%AB/tabid/164/language/zh-TW/Default.aspx`.

[28] Z.-L. LU and U H. LOK, *Supplementary material of the paper Z.-L Lu and U H. Lok, "Dimension-Reduced Modeling for Local Volatility Surface via Unsupervised Learning"*, Romanian Journal of Information Science and Technology, 2024. Accessed: Jun. 5, 2024. [Online]. Available: https://reurl.cc/ezaez7.